Low-Temperature Chemical Vapor Deposition Growth of Graphene from Toluene on Electropolished Copper Foils

Bin Zhang,[†,‡] Wi Hyoung Lee,[†] Richard Piner,[†] Iskandar Kholmanov,[†] Yaping Wu,[†] Huifeng Li,[†] Hengxing Ji,[†] and Rodney S Ruoff[†,*]

[†]Department of Mechanical Engineering and the Materials Science and Engineering Program, The University of Texas at Austin, One University Station C2200, Austin, Texas 78712-0292, United States and [‡]Key Laboratory for Anisotropy and Texture of Materials of Ministry of Education, School of Materials and Metallurgy, Northeastern University, Shenyang 110819, People's Republic of China

Simple, controllable, and economical methods of growing large-area, high-quality, continuous, and uniform monolayer graphene are a prerequisite for a wide range of applications of graphene. Chemical vapor deposition (CVD) growth of graphene on the surface of a Cu substrate[1,2] is the most promising method to date for the growth of large-area monolayer graphene, owing to the extremely low solubility of C in Cu.[3] Typically, growth of graphene by CVD has used methane as the precursor[1,2,4] and growth temperatures of around 1000 °C. Although a Au–Ni alloy catalyst can grow graphene at 450 °C, only 74% monolayer graphene was obtained, and by Raman mapping, the D peaks were higher than the G peaks around the domain edges.[5] Recent reports[6–9] indicate that the temperature of graphene growth with several other carbon sources can be less than 1000 °C, such as hexane-derived continuous graphene films grown at 950,[8] 975, and 900 °C,[9] ethanol or pentane-derived graphene grown at 900 °C,[6] alcohol-derived graphene at temperatures ranging from 650 to 850 °C,[7] and under low-pressure CVD (LPCVD) or ambient-pressure CVD, respectively. The "graphene" grown at 650 °C[7] had a D peak intensity much higher than that of the G peak in the reported Raman spectrum. The lowest growth temperature reported to date was 300 °C with benzene by LPCVD in which[10] graphene flakes were obtained but not continuous graphene films.

In addition, many groups have been using Cu foils from Alfa-Aesar after the work reported by Li et al.[1] We have found that these foils are typically covered by the supplier with a layer of chromium oxide for anticorrosion protection. Moreover, the surface roughness of the

ABSTRACT
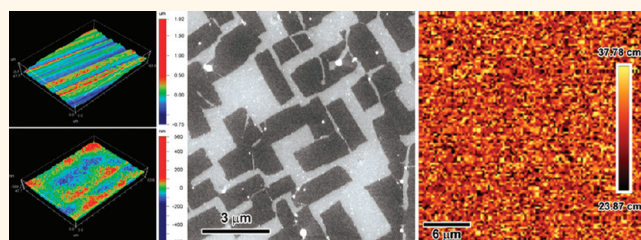
A two-step CVD route with toluene as the carbon precursor was used to grow continuous large-area monolayer graphene films on a very flat, electropolished Cu foil surface at 600 °C, lower than any temperature reported to date for growing continuous monolayer graphene. Graphene coverage is higher on the surface of electropolished Cu foil than that on the unelectropolished one under the same growth conditions. The measured hole and electron mobilities of the monolayer graphene grown at 600 °C were 811 and 190 cm^2/(V·s), respectively, and the shift of the Dirac point was 18 V. The asymmetry in carrier mobilities can be attributed to extrinsic doping during the growth or transfer. The optical transmittance of graphene at 550 nm was 97.33%, confirming it was a monolayer, and the sheet resistance was ~8.02 × 10^3 Ω/□.

Cu substrate is expected to be a factor influencing homogeneity and electronic transport properties of the graphene due to the growth terminating in the irregular "valleys" of the substrate surface.[11,12]
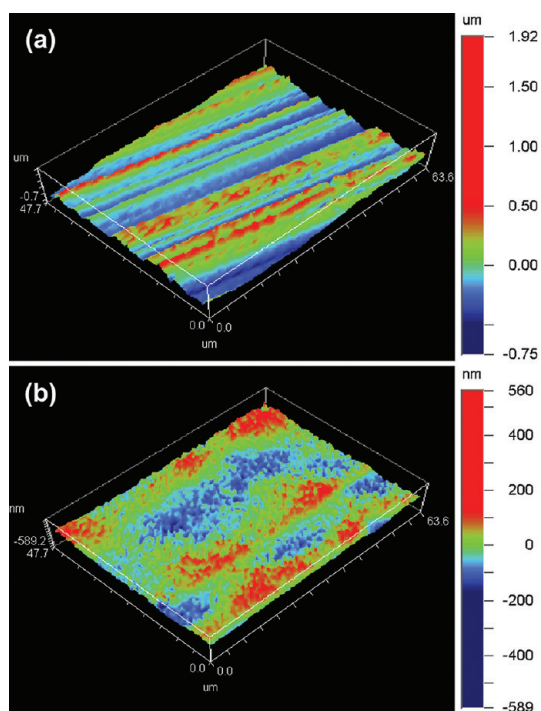
Here, we report using toluene and LPCVD to grow continuous monolayer graphene films at 500 to 600 °C on flat and electropolished Cu foils and by a two-step growth method. The Raman spectra, electron and hole mobilities, sheet resistance, and optical transmittance of the graphene were measured and are reported below.

Figure 1. Optical surface profiler images and the calculated roughness of the Cu foil substrates (a) before and (b) after electropolishing.

RESULTS AND DISCUSSION

A flat and smooth Cu foil was achieved by electropolishing (see Methods). Figure 1a,b shows the surface of the Cu foils before and after electropolishing as measured by an optical profilometer. The Cu foils were produced by cold rolling, and their surfaces have straight striations with spacing of a few micrometers (Figure 1a). The electropolished Cu surface is much smoother, and the striations have been removed, as shown in Figure 1b (also see Figure S1a,b in Supporting Information). A measurement of the root-mean-square (rms) surface roughness, R_q (see Supporting Information), showed that R_q was reduced from 218.56 nm for the as-received Cu foil to 64.00 nm for the electropolished one. The electropolishing thus "flattens" the Cu foil surface and removes metal oxides. In order to remove oxide layers prior to graphene growth, our team has tried hydrochloric acid or acetic acid etching and mechanical polishing. However, electropolishing the metal substrate for graphene growth is rarely reported,[11] even though it is a widely used method in metal research. Our procedure is different from the method reported by Luo et al.,[11] as we present a simple method to electropolish the Cu foils in 1 min (see Methods).

After 980 °C annealing in hydrogen under low pressure, the Cu foils were exposed to toluene. The weakest bond in toluene is the C—H bond in the methyl group, whose bond energy is 324 kJ/mol,[13] while the bond energy of the C—H bond in benzene is 460 kJ/mol. This consideration motivated our choice of toluene, along with the fact that it is considerably less toxic than benzene. To observe the morphology of graphene domains (islands) prior to formation of a full monolayer, growth was interrupted at various times (batch experiments). Figure 2a—d shows typical SEM images of the graphene flakes grown on electropolished Cu foils at different temperatures after a 30 min one-step growth (without using a second step that is described below). With a growth temperature of 300 °C, sparse domains are observed on the Cu foil surface, whereas more graphene domains per unit area are observed for the 400 °C growth. Domains grown at 500 and 600 °C (Figure 2c,d) have a rectangular shape. The corresponding Raman spectra (Figure 2e) show features typical of monolayer graphene.[14,15] The 2D band centered at ~2691 cm^{-1} is symmetric; the full width at half-maximum (fwhm) of the 2D peak is ~39 cm^{-1}, and the intensity ratio of the G band to the 2D band (I_G/I_{2D}) is ~0.5. The size of the rectangular domains grown at 600 °C is larger than that grown at 500 °C after the same 30 min growth. The rectangular shape is different from the shapes typically seen, such as the four- or six-lobe shape of methane-derived graphene domains[16] grown at 1035 °C under low pressure , the hexagonal shapes of methane-derived domains grown at 1050 °C[17] at ambient pressure, and the benzene-derived domains grown at 500 °C under low pressure.[10] The rectangular graphene might be related to the partial pressure of the hydrogen in the reactors. Hydrogen might play an important role in etching edges and corners of the graphene flakes under proper growth conditions. Comparing the partial pressure of hydrogen reported in the literature[10,16,17] and the present results, the higher the partial pressure of hydrogen, the easier the domain shapes tend to be equiaxed shape due to more sharp edges and corners of the graphene flakes etched. This means that sharp four- or six-lobe domains can grow under lower partial pressure of hydrogen and the hexagonal domains under higher hydrogen partial pressure. The partial pressure of hydrogen for the present rectangular domains is between them.

The Cu foils used for the catalyst growth of different domain shapes are the same sort of Alfa-Aesar foils, which tend to have the same grain orientations after annealing.[18] Figure 2f presents a typical EBSD map of our annealed Cu foil covered with graphene domains. The corresponding inverse pole figure is also shown in the right part of the Figure 2f. It can be seen that most grains on the surface of the annealed Cu foil have (001) planes. Our result is consistent with the well-accepted fact that recrystallization would result in the formation of an ⟨001⟩ texture component when a cold-rolled Cu is annealed above the recrystallization temperature. This tendency is commonly reported in the literature related to metal
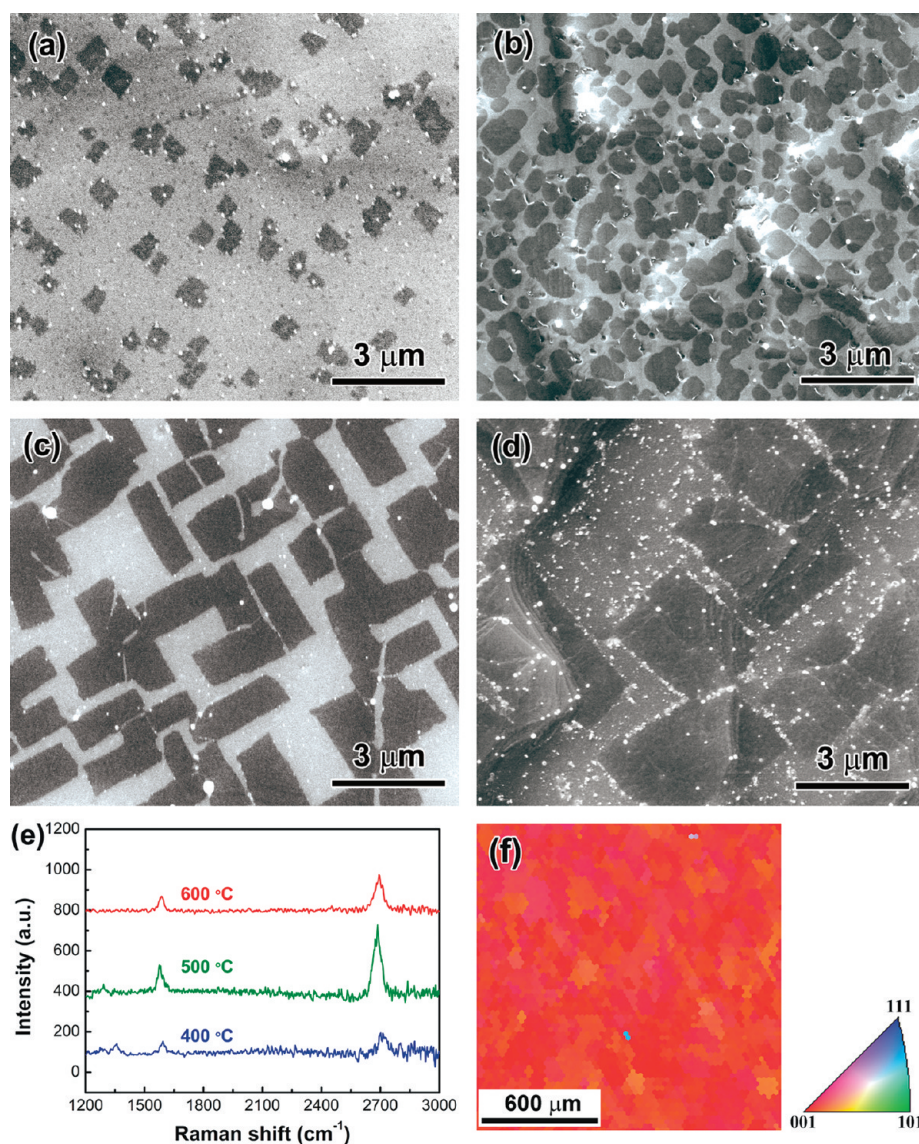
Figure 2. SEM images of graphene domains grown at the temperatures of (a) 300 °C, (b) 400 °C, (c) 500 °C, and (d) 600 °C. (e) Corresponding Raman spectra of the graphene flakes on Cu foils; (f) EBSD map of the Cu foil annealed at 980 °C followed by growth of graphene domains at 600 °C and its corresponding inverse pole figure.

cold-working. For example, Dai et al.[18] reported that, after having been annealed at high temperature, Cu foil had a strong ⟨001⟩ texture; that is, most of the grains in the foils tend to have an out-of-plane orientation close to ⟨001⟩. Our (001)-oriented grains at the foil surface actually became preferential sites for the more uniform growth of graphene, as shown in Figure 2a–d. Furthermore, it is worth noting that only rectangular domains were observed by SEM. This indicates that there is not a close relationship between the domain shape and the underlying Cu grain orientation under our growth conditions. In addition, we have performed a two-step growth process first developed in our group for the growth of methane-derived graphene at higher temperature.[16] A low graphene nuclei density is first created under lower chamber pressure, followed by

achieving full graphene surface coverage by increasing the chamber pressure by a factor of 10.

Figure 3a is a SEM image of a continuous graphene film grown on electropolished Cu foil at 600 °C after 1 h exposure to toluene using our two-step growth process. The clear presence of Cu surface steps throughout indicates that graphene completely covers the Cu surface. Figure 3b shows a graphene film transferred to a Si/SiO$_2$ substrate (285 nm thick oxide) and an optical image taken with a 100× objective lens in the Raman spectroscope. The image taken with the 100× objective lens reveals that the graphene film is continuous and uniform, and no wrinkles are observed. The Raman spectrum in Figure 3c is that of monolayer graphene,[14,15] with an intensity ratio of the 2D to G band of about 2.18 and a symmetric 2D band at ∼2700 cm^{-1} with a fwhm of ∼36 cm^{-1}. The D band
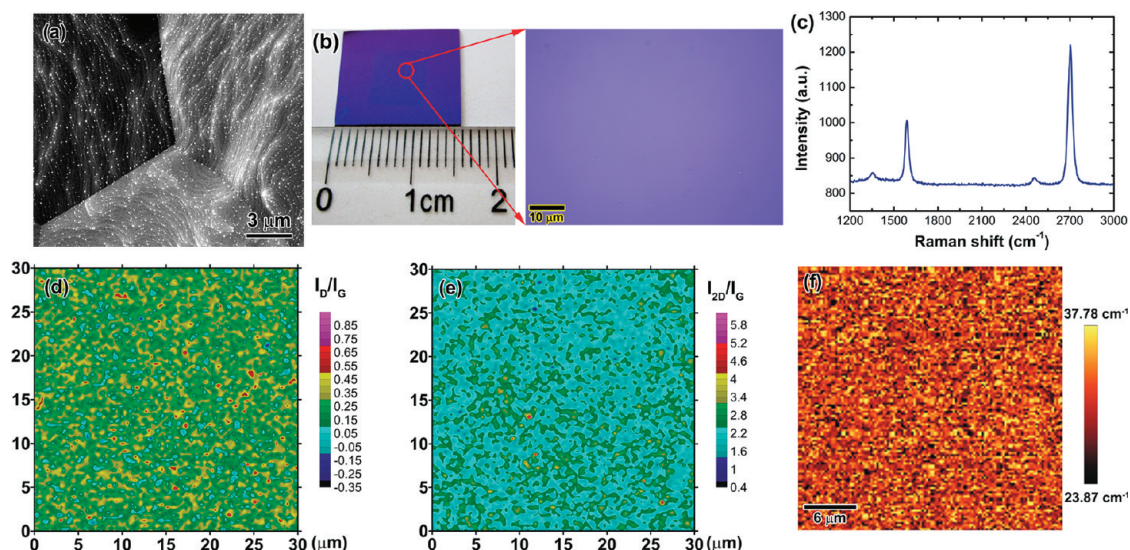
Figure 3. Toluene-derived continuous graphene films grown at 600 °C. (a) SEM image of the graphene on the electropolished Cu surface. (b) Optical image of the graphene transferred onto a Si/SiO$_2$ substrate and an image taken under Raman 100× lens (λ = 488 nm). (c) Typical Raman spectrum of the graphene. (d,e) Raman maps of the intensity ratio of the D band (1300−1400 cm^{-1}) to the G band (1540−1640 cm^{-1}) and the 2D band (2640−2760 cm^{-1}) to the G band, respectively. (f) Raman map of fwhm of the 2D band (measured over 30 × 30 μm^2 area).

is observed at ∼1350 cm^{-1}, suggesting the presence of disordered structural defects, which might be present at the domain boundaries of the graphene. Sample uniformity was confirmed by confocal Raman spectroscopy mapping over 30 × 30 μm^2 areas of the graphene on Si/SiO$_2$. Measured maps of the intensity ratio of D band (region from 1300 to 1400 cm^{-1}) to G band (1540 to 1640 cm^{-1}), the 2D band (2640 to 2760 cm^{-1}) to the G band (I_{2D}/I_G), and the fwhm of the 2D band are presented in Figure 3d−f, respectively. Figure 3f presents the fwhm map of the 2D band in the range of 23.87−37.78 cm^{-1}, which indicates that the graphene films are monolayer. These data are also consistent with the Raman map of I_{2D}/I_G (Figure 3e). Most areas of Figure 3e are light blue/green, which show I_{2D}/I_G in the range of 2.0−3.0, characteristic of monolayer graphene. At one point of the map, the ratio is less than 1. As to the reason why we never observed wrinkles of our graphene, which are typically attributed to the different thermal expansion coefficients between Cu and graphene,[1] some may arise due to hydrogen dissolved in Cu foils degassing at elevated temperature.[19] The solubility of H$_2$ gas in Cu at 1000 °C is ∼7 × 10^{-3} atom %,[19,20] while this value is much lower, namely, ∼7 × 10^{-5}, at 600 °C. At room temperature, the solubility of hydrogen declines to less than 10^{-7} atom %.[20] It is possible that hydrogen is dissolving into the copper during the annealing step, then leaving the copper after the graphene is formed. By growing at lower temperature, most of the dissolved hydrogen has perhaps already left the copper before the graphene is formed, which could be useful if evolution of H$_2$(g) from the Cu is playing a role in, for example, the presence of wrinkles.
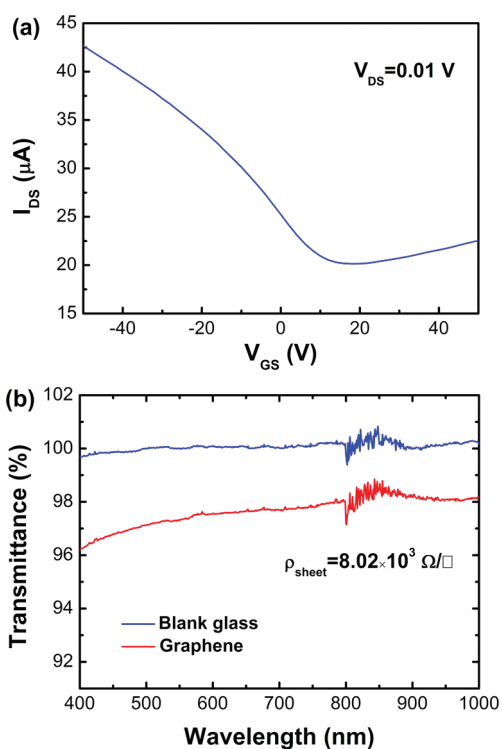
Figure 4. (a) Graphene FET used for carrier mobility measurement. The channel width and length between the two Cr/Au contacts were 300 and 50 μm, respectively. I_{DS} vs V_{GS} curve for a fixed V_{DS} = 0.01 V. V_{GS} scans from −50 to 50 V. (b) Transmittance of the graphene film from 350 to 1000 nm. The transmittance at 550 nm is 97.33%, and the sheet resistance (ρ_{sheet}) of the graphene is ∼8.02 × 10^3 Ω/□.

In addition, we also tried unelectropolished Cu foils without the anticorrosion coating and compared it with the electropolished ones. After the same 45 min growth at 550 °C, graphene coverage on the

unpolished Cu foil is much lower than that of the electropolished one, although graphene can also grow on it (see Figure S3 in Supporting Information).

We fabricated a back-gated FET with graphene grown at 600 °C (see Methods and Supporting Information). The graphene channel width and length were 300 and 50 μm, respectively. Devices were measured at room temperature under ambient conditions. The I_{DS} versus V_{GS} (the gate voltage) curve (Figure 4a) measured at a source−drain bias (V_{DS}) of 0.01 V shows that the gate can cause either hole or electron conduction. The Dirac point voltage is at $V_{GS} \sim 18$ V. The mobilities were calculated to be hole mobility $\mu_h = 811$ cm^2/(V·s) and electron mobility $\mu_e = 190$ cm^2/(V·s). The asymmetry[21,22] in carrier mobility of the device may be attributed to the extrinsic doping during the growth, transfer, and/or the adsorption of air molecules during the measurement process under ambient conditions. The same type of graphene (8×8 mm^2) was transferred to a glass slide, and the same glass was used as a reference. The transmittance at 550 nm wavelength is 97.33% (Figure 4b), which is comparable to that reported, 97.7%, for high-temperature CVD monolayer graphene.[23] The sheet resistance of the same graphene was $\sim 8.02 \times 10^3$ Ω/□. The sheet resistance and the carrier mobilities are "worse" than that of graphene grown by our team with methane at higher temperature ($1.00-4.00 \times 10^3$ Ω/□ and ~ 4000 cm^2/(V·s), respectively). This may result from the increased density of grain boundaries and/or defects of graphene grown at the low temperature.

Although the carrier mobilities and the sheet resistance of our graphene films, so far, are worse than that of graphene grown by our team with methane and typical strategies at higher temperature, the feasibility of graphene grown at low temperature demonstrated here has a wider significance for the lower energy consuming growth of large-scale graphene. Moreover, it is expected that the CVD graphene grown at low temperature might be transferred more easily due to the weaker coupling to the metal substrate, which may be beneficial for developing other transfer methods. Further work to optimize growth at low temperatures with various hydrocarbon precursors is indicated. The carrier mobilities and the sheet resistance of our graphene films can be further improved by crack-free transfer[24] and/or graphene doping.

CONCLUSION

Uniform and continuous monolayer graphene films have been grown on electropolished copper foils at 600 °C with LPCVD using toluene and hydrogen. The flat electropolished Cu foils help in growing uniform and large graphene domains. A second growth step (increasing chamber pressure by a factor of 10 to complete a full film) is a key factor that allows completing the coverage of graphene on the Cu surface. Electron and hole mobilities of 811 and 190 cm^2/(V·s), respectively, were measured; the transmittance of graphene at 550 nm was 97.33%, and the sheet resistance of the same graphene was 8.02×10^3 Ω/□.

METHODS

Electropolishing of Copper Foils. Used as an anode, 25 μm thick Cu foil (99.8%, Alfa-Aesar, item no. 13382) was electropolished in a homemade electrochemistry cell with a large Cu plate as the cathode; the electropolishing solution was 1000 mL of water, 500 mL of *ortho*-phosphoric acid, 500 mL of ethanol, 100 mL of isopropyl alcohol, and 10 g of urea. Supported by an alligator clip, the Cu foil was placed into the solution. A Hewlett-Packard 6612 System DC power supply was used to supply constant voltage/current, and a voltage in the range of 3.0−6.0 V was applied for 60 s. After electropolishing, the Cu foil was rinsed with deionized water, further washed with ethanol, and then blow-dried with nitrogen.

Graphene Growth with Toluene. Electropolished Cu foils were inserted into a 22 mm i.d. quartz tube, heated by a horizontal split-tube furnace. The toluene was loaded in a homemade container which is isolated from the main system with a valve. First, the quartz tube was pumped down to 10^{-2} Torr, and then ultrahigh purity grade hydrogen (Air Gas Inc.) was introduced during temperature ramp-up of the furnace (pressure $\sim$370 mTorr, flow rate of $\sim$3.3 sccm (STP flow rate)). The Cu foils were annealed at 980 °C in hydrogen for 15 min. After annealing, the furnace was cooled to the desired growth temperature, 300, 400, 500, or 600 °C. A schematic of the LPCVD system is in Figure S1. When the desired temperature was achieved, the valve to the toluene was opened. Toluene vapor was passed into the quartz tube at a flow rate of 2.7 mL/h to maintain a toluene partial pressure of $\sim$300 mTorr without

changing the flow rate of hydrogen. The typical growth time was 60 min at each of the four temperatures studied. For the second growth step (that causes islands (domains) to continue to grow and merge into a complete film), 5 min before finishing the growth, the ball valve between the quartz tube outlet and the pump was closed, so that the pressure increased by a factor of 10 without changing any other parameters. The furnace was then cooled to the 200−300 °C range at a rate of $\sim$50 °C/min. Toluene was then turned off, while hydrogen continued flowing until the furnace cooled to room temperature.

Graphene Transfer. When the copper foil is electropolished, both sides are polished at the same time. So, graphene was found on both sides of the Cu foil. However, we usually keep the graphene grown on the side facing the counter electrode, and this side was spin-coated (4000 rpm $\times$ 40 s) with a layer of poly(methyl methacrylate)[25] (PMMA) (MW 350 000; 46 mg/mL in chlorobenzene). After the Cu foil was dipped in an aqueous $(NH4)_2S_2O_8$ solution (0.5 M) for 20 min, the graphene on the other side of the Cu foil was removed by "washing it off" using deionized water. Then, after the Cu substrate was completely dissolved in the aqueous $(NH4)_2S_2O_8$ solution, the PMMA−graphene was transferred onto Si substrates covered with 285 nm thick SiO_2 (Si/SiO$_2$ substrate) or glass slides. The samples were dried in air for 30 min and then under vacuum (10^{-2} Torr) for 30 min in order to remove water between graphene and the substrate. Subsequently, PMMA was removed using acetone.

Characterization. Scanning electron microscopy (SEM) images were obtained using an FEI Quanta-600 FEG-ESEM at an

accelerating voltage of 30 kV. Raman spectroscopy was done with a WITec alpha 300 confocal Raman spectroscope with a laser wavelength of 488 nm and a 100× objective lens (laser spot size is 300 nm). Scanning with this instrument was used to evaluate the quality and uniformity of graphene on a Si/SiO$_2$ substrate. A wide range of surface roughness of the Cu foils before and after electropolishing trials was measured by a noncontact optical profiler (Wyko Surface Profiler) in vertical scanning interferometry (VSI) mode. An electron backscattering diffraction (EBSD) analysis was conducted in a Zeiss Neno 40 FE-SEM to obtain a grain orientation map of the Cu foil covered with graphene domains. FET measurements were performed with a programmable voltage source (Keithley 2611A and Keithley 6221 digital voltmeter and 6514 digital ammeter) at room temperature under ambient atmosphere. The electrical resistance of the graphene films was measured by the van der Pauw method.[26] A spectroscopic ellipsometer (JA Woolam, M-2000) was used for the measurement of the transmittance of the graphene films, and a bare glass slide was used as a reference.

Conflict of Interest: The authors declare no competing financial interest.

Supporting Information Available: The schematic of the CVD setup for growing continuous graphene films and their additional roughness, SEM, and FET characterization. This material is available free of charge *via* the Internet at http://pubs.acs.org.

REFERENCES AND NOTES

1. Li, X.; Cai, W.; An, J.; Kim, S.; Nah, J.; Yang, D.; Piner, R.; Velamakanni, A.; Jung, I.; Tutuc, E.; *et al.* Large-Area Synthesis of High-Quality and Uniform Graphene Films on Copper Foils. *Science* **2009**, *324*, 1312–1314.

2. Bae, S.; Kim, H.; Lee, Y.; Xu, X.; Park, J.-S.; Zheng, Y.; Balakrishnan, J.; Lei, T.; Ri Kim, H.; Song, Y. I.; *et al.* Roll-to-Roll Production of 30-in. Graphene Films for Transparent Electrodes. *Nat. Nanotechnol.* **2010**, *5*, 574–578.

3. Lopez, G. A.; Mittemeijer, E. J. The Solubility of C in Solid Cu. *Scr. Mater.* **2004**, *51*, 1–5.

4. Li, X.; Magnuson, C. W.; Venugopal, A.; Tromp, R. M.; Hannon, J. B.; Vogel, E. M.; Colombo, L.; Ruoff, R. S. Large-Area Graphene Single Crystals Grown by Low-Pressure Chemical Vapor Deposition of Methane on Copper. *J. Am. Chem. Soc.* **2011**, *133*, 2816–2819.

5. Weatherup, R. S.; Bayer, B. C.; Blume, R.; Ducati, C.; Baehtz, C.; Schlögl, R.; Hofmann, S. *In Situ* Characterization of Alloy Catalysts for Low-Temperature Graphene Growth. *Nano Lett.* **2011**, *11*, 4154–4160.

6. Dong, X.; Wang, P.; Fang, W.; Su, C.-Y.; Chen, Y.-H.; Li, L.-J.; Huang, W.; Chen, P. Growth of Large-Sized Graphene Thin-Films by Liquid Precursor-Based Chemical Vapor Deposition under Atmospheric Pressure. *Carbon* **2011**, *49*, 3672–3678.

7. Guermoune, A.; Chari, T.; Popescu, F.; Sabri, S. S.; Guillemette, J.; Skulason, H. S.; Szkopek, T.; Siaj, M. Chemical Vapor Deposition Synthesis of Graphene on Copper with Methanol, Ethanol, and Propanol Precursors. *Carbon* **2011**, *49*, 4204–4210.

8. Srivastava, A.; Galande, C.; Ci, L.; Song, L.; Rai, C.; Jariwala, D.; Kelly, K. F.; Ajayan, P. M. Novel Liquid Precursor-Based Facile Synthesis of Large-Area Continuous, Single, and Few-Layer Graphene Films. *Chem. Mater.* **2010**, *22*, 3457–3461.

9. Yao, Y. G.; Li, Z.; Lin, Z. Y.; Moon, K. S.; Agar, J.; Wong, C. P. Controlled Growth of Multilayer, Few-Layer, and Single-Layer Graphene on Metal Substrates. *J. Phys. Chem. C* **2011**, *115*, 5232–5238.

10. Li, Z.; Wu, P.; Wang, C.; Fan, X.; Zhang, W.; Zhai, X.; Zeng, C.; Li, Z.; Yang, J.; Hou, J. Low-Temperature Growth of Graphene by Chemical Vapor Deposition Using Solid and Liquid Carbon Sources. *ACS Nano* **2011**, *5*, 3385–3390.

11. Luo, Z.; Lu, Y.; Singer, D. W.; Berck, M. E.; Somers, L. A.; Goldsmith, B. R.; Johnson, A. T. C. Effect of Substrate Roughness and Feedstock Concentration on Growth of Wafer-Scale Graphene at Atmospheric Pressure. *Chem. Mater.* **2011**, *23*, 1441–1447.

12. Wellmann, R.; Bottcher, A.; Kappes, M.; Kohl, U.; Niehus, H. Growth of Graphene Layers on HOPG *via* Exposure to Methyl Radicals. *Surf. Sci.* **2003**, *542*, 81–93.

13. Szwarc, M. The C–H Bond Energy in Toluene and Xylenes. *J. Chem. Phys.* **1948**, *16*, 128–136.

14. Andrea, C, F. Raman Spectroscopy of Graphene and Graphite: Disorder, Electron–Phonon Coupling, Doping and Nonadiabatic Effects. *Solid State Commun.* **2007**, *143*, 47–57.

15. Malard, L. M.; Pimenta, M. A.; Dresselhaus, G.; Dresselhaus, M. S. Raman Spectroscopy in Graphene. *Phys. Rep.* **2009**, *473*, 51–87.

16. Li, X.; Magnuson, C. W.; Venugopal, A.; An, J.; Suk, J. W.; Han, B.; Borysiak, M.; Cai, W.; Velamakanni, A.; Zhu, Y.; *et al.* Graphene Films with Large Domain Size by a Two-Step Chemical Vapor Deposition Process. *Nano Lett.* **2010**, *10*, 4328–4334.

17. Yu, Q.; Jauregui, L. A.; Wu, W.; Colby, R.; Tian, J.; Su, Z.; Cao, H.; Liu, Z.; Pandey, D.; Wei, D.; *et al.* Control and Characterization of Individual Grains and Grain Boundaries in Graphene Grown by Chemical Vapor Deposition. *Nat. Mater.* **2011**, *10*, 443–449.

18. Dai, C. Y.; Zhang, G. P.; Yan, C. Size Effects on Tensile and Fatigue Behaviour of Polycrystalline Metal Foils at the Micrometer Scale. *Philos. Mag.* **2011**, *91*, 932–945.

19. Gao, L.; Ren, W.; Zhao, J.; Ma, L. P.; Chen, Z.; Cheng, H. M. Efficient Growth of High-Quality Graphene Films on Cu Foils by Ambient Pressure Chemical Vapor Deposition. *Appl. Phys. Lett.* **2010**, *97*, 183109-3.

20. Fromm, E; Jehn, H. Solubility of Hydrogen in the Elements. *Bull. Alloy Phase Diagrams* **1984**, *5*, 323–325.

21. Chen, J. -H.; Jang, C.; Adam, S.; Fuhrer, M. S.; Williams, E. D.; Ishigami, M. Charged-Impurity Scattering in Graphene. *Nat. Phys.* **2008**, *4*, 377–381.

22. Novikov, D. S. Numbers of Donors and Acceptors from Transport Measurements in Graphene. *Appl. Phys. Lett.* **2007**, *91*, 102102.

23. Li, X. S.; Cai, W. W.; Jung, I. H.; An, J. H.; Yang, D. X.; Velamakanni, A.; Piner, R.; Colombo, L.; Ruoff, R. S. Synthesis, Characterization, and Properties of Large-Area Graphene Films. *ECS Trans.* **2009**, *19*, 41–52.

24. Suk, J. W.; Kitt, A.; Magnuson, C. W.; Hao, Y.; Ahmed, S.; An, J.; Swan, A. K.; Goldberg, B. B.; Ruoff, R. S. Transfer of CVD-Grown Monolayer Graphene onto Arbitrary Substrates. *ACS Nano* **2011**, *5*, 6916–6924.

25. Morozov, S. V.; Novoselov, K. S.; Katsnelson, M. I.; Schedin, F.; Elias, D. C.; Jaszczak, J. A.; Geim, A. K. Giant Intrinsic Carrier Mobilities in Graphene and Its Bilayer. *Phys. Rev. Lett.* **2008**, *100*, 016602.

26. Pauw, L. J. V. D. A Method of Measuring the Resistivity and Hall Coefficient on Lamellae of Arbitrary Shape. *Philips Tech. Rev.* **1958**, *20*, 220–224.